Materials Letters 335 (2023) 133830

Contents lists available at ScienceDirect

Materials Letters

journal homepage: www.elsevier.com/locate/matlet

Development of activated carbon by bio waste material for application in supercapacitor electrodes

Raman Devi [a], Vinay Kumar [a,*], Sunil Kumar [a], Avnish Kumar Sisodiya [b], Ajay Kumar Mishra [c,d], Anushree Jatrana [e], Ashwani Kumar [f], Paul Singh [a]

[a] Department of Physics, COBS&H, CCS Haryana Agricultural University, Hisar, Haryana 125004, India
[b] Department of Physics, Motilal Nehru College, University of Delhi South Campus, New Delhi 110021, India
[c] College of Pharmaceutical and Chemical Engineering, Hebei University of Science and Technology, Shijiazhuang, 050018, China
[d] Department of Chemistry, Durban University of Technology, Steve Biko Road, 4001 Durban, South Africa
[e] Department of Chemistry, COBS&H CCS Haryana Agricultural University, Hisar, Haryana, 125004, India
[f] Nanoscience Laboratory, Institute Instrumentation Centre, IIT Roorkee, Uttrakhand 247667, India

ARTICLE INFO

Keywords:
Activated carbon
Hydrothermal
Biowaste
Supercapacitor
Electrode

ABSTRACT

Green nanotechnology is now emerging to address society's global sustainability issues by recycling numerous industrial and bio-wastes to produce functional carbonaceous nanomaterials like biochar, 2D graphene, graphene oxide, carbon nanotube (CNT), activated carbon (AC), etc. In this study, we have synthesized AC via the hydrothermal decomposition approach of the walnut shell under high temperature and pressure in a hydrothermal autoclave at temperature ranges from 200 to 250 °C. The synthesized AC has a high specific surface area of 408.8 m^2/g. It has an excellent specific capacitance of 204F/g at 1 A/g of current density with good cyclability up to 10,000 cycles.

1. Introduction

The growing population, depletion of fossil fuels, and environmental threat require advancement in energy storage. Therefore, it is highly desired for researchers to develop an effective way of providing alternate sources of energy and conversion technologies. There are many alternative renewable energy sources that can replace the need for fossil fuels. Solar, wind, geothermal and biomass-based energy are a few examples of alternative energy sources currently being investigated [1]. In addition, biomass-derived nanomaterials are a clean and effective energy source for supercapacitors. Electrochemical capacitors (ECs), also known as supercapacitors, have attracted much interest in the advanced energy storage area due to their extensive cycle life, long-term durability, and outstanding specific power [2]. Supercapacitors are classified into two categories based on charge-storage mechanisms: pseudocapacitors and electric double-layer capacitors (EDLCs) [3].

Carbon-derived materials are the most intriguing electrode for EDLCs, such as graphene, CNT, graphene oxide, carbon black, etc., because of their excellent mechanical strength, good-electrical conductivity, and higher surface-to-volume ratio. However, these materials are hard to synthesize and require harsh chemical conditions for massive production. In this regard, AC has a highly active surface, easily tunable porosity, and excellent electrical conductivity; bio-carbon produced from bio-waste materials is a promising electrode candidate for EDLCs [4]. There are different methods for preparing AC, such as pyrolysis, hydrothermal carbonization, and gasification. The hydrothermal method is preferred over others due to its low cost, low-temperature conditions, and high yield. Over the past few years, many precursors have been successfully converted into AC to obtain excellent specific capacitance and better understand the physical phenomenon between the electrode–electrolyte interfaces in EDLCs [5]. As a result, selecting an adequate precursor for the synthesis of low-cost, eco-friendly, and livable AC is a problematic issue for researchers in this field. In this regard, walnut shell renewable biomass being cheaper, abundant, clean, and sustainable, shows considerable potential as an AC precursor [6].

2. Experimental

2.1. Preparation of AC

Firstly, walnut shells were washed multiple times with DI water,

* Corresponding author.
E-mail address: vinay23@hau.ac.in (V. Kumar).

https://doi.org/10.1016/j.matlet.2023.133830
Received 9 September 2022; Received in revised form 7 December 2022; Accepted 4 January 2023
Available online 6 January 2023

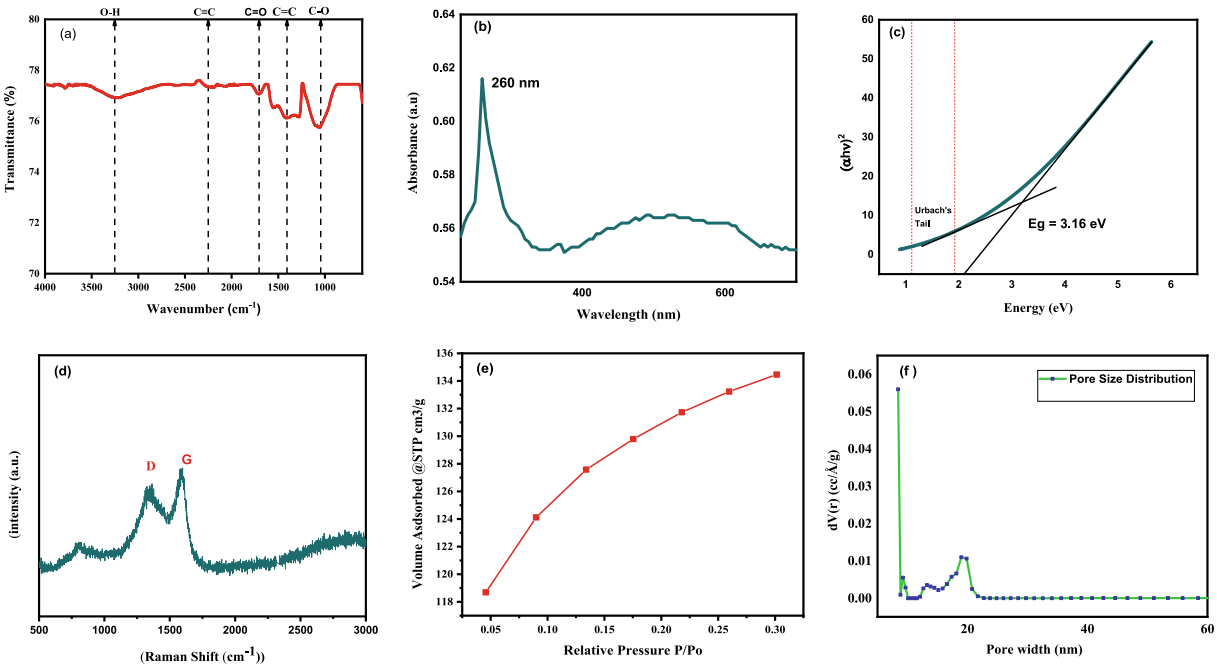

Fig. 1. (a) FTIR spectra of AC, (b) UV–vis spectra, (c) Tauc's plot, (d) Raman Spectra, (e)N_2 adsorption–desorption isotherms, (f) Pore size distribution curve.

dried overnight at 105 °C in the oven, and ground into fine powder. Then, 8 g of raw walnut shell powder was mixed with 80 ml of distilled water and placed in an autoclave at 225 °C (6 h). The sample was rinsed many times with DI water and then oven-dried for 12 h at 105 °C. Further, the obtained product was impregnated with KOH in the proportion of 1:3 and then dried for 12 h. Then the final product was obtained by annealing at 450 °C for 2 h at a ramp rate of 10 degrees per minute.

2.2. Electrochemical analysis

The working electrode was fabricated by mixing the active material (AC, 90 wt%) with the PVDF binder (10 wt%) in an organic solvent (*N*-methyl pyrrolidinone). The mixture mentioned above was agitated on a magnetic stirrer, yielding a homogeneous slurry, which was then applied to the graphite sheet (working electrode). The coated electrodes were annealed for 24 h at 70 °C in a vacuum oven. The capacitive behavior of the electrode was evaluated using cyclic voltammetry (CV) in 6 M KOH as an electrolyte with diverse scan-rate varies from 25 to 200 m Vs^{-1}. Electrochemical impedance spectroscopy (EIS) was studied in the frequency range of 100 kHz to 10 MHz. Galvanostatic Charging Discharging (GCD) was investigated at varied current densities ranging from 1 to 10 A/g.

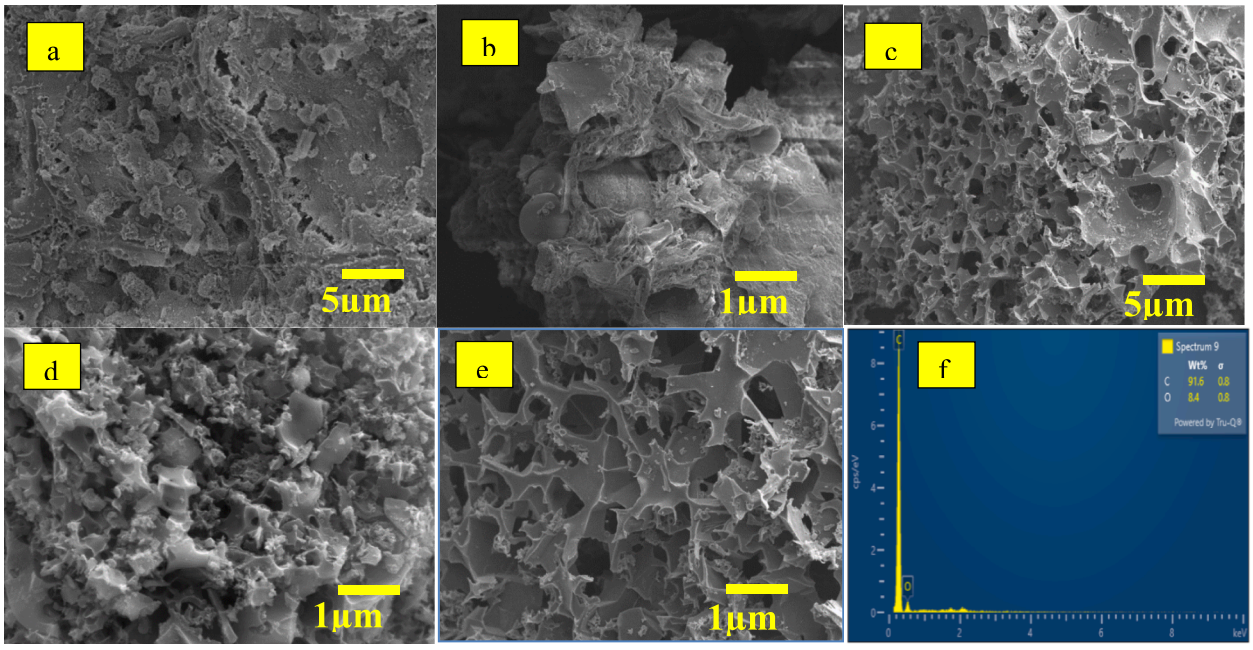

Fig. 2. (a, b) FE-SEM image before activation, (c, d) FE-SEM images of AC after activation, (e, f) EDX analysis.

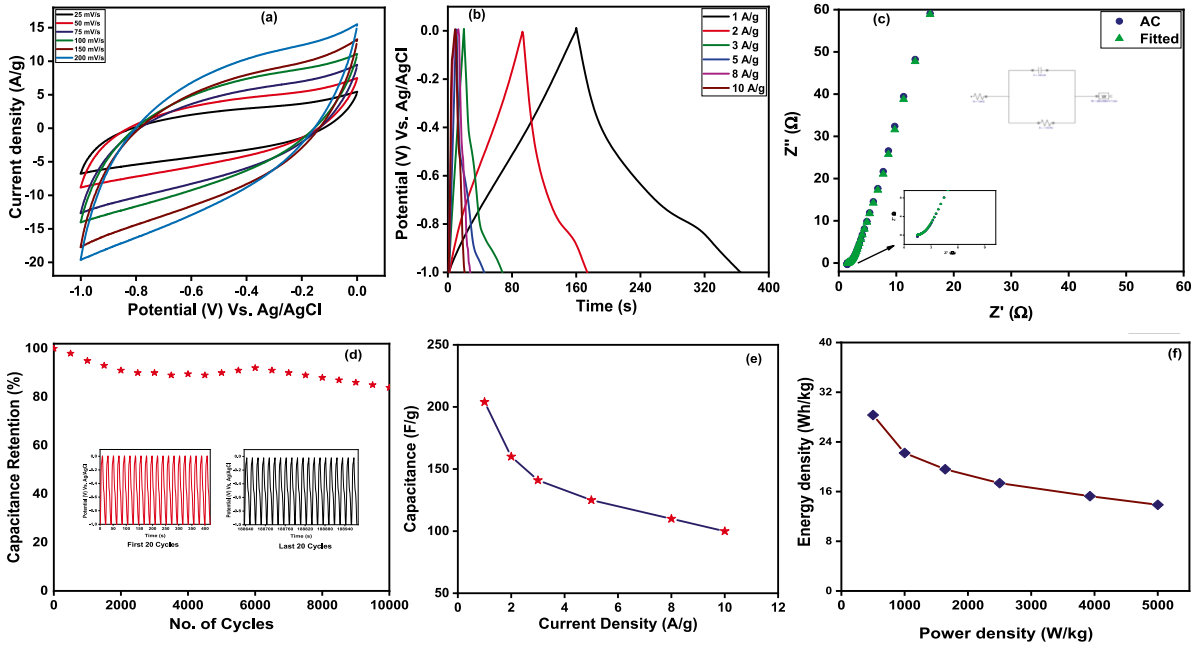

Fig. 3. Electrochemical performance measurements;(a) CV analysis at 25 to 200 mVs^{-1}, (b) GCD plot, (c) Nyquist plot, (d) Capacitive retention vs cycle number, (e) Variation in Sp. Capacitance vs current density, (f) Ragone plot.

3. Results and discussion

The IR spectra for AC, from 4000 to 400 cm^{-1}, are shown in Fig. 1 (a). A substantial broad and strong peak between 3550 and 3200 cm^{-1} indicates OH group stretching vibration. Another peak was noticed at 2249.6 cm^{-1}, indicating C≡C stretching vibration from an aromatic group. Peaks at 1704 cm^{-1} are expected to be carboxyl group stretching vibrations [7].

Fig. 1(b) represents the UV–Visible spectra of the AC. In this spectrum, the absorbance of radiation by the sample is plotted against the wavelength of light. By using this spectrum, the optical properties of the material were analyzed. The highest absorbance peak at 260 nm was obtained. To compute the sample's direct band gap, Tauc's plot of energy v/s $(\alpha hv)^2$ was examined, represented in Fig. 1(c) [8]. The calculated band gap for the AC is 3.16 eV [9]. The AC's N2 adsorption/desorption isotherm BET plot is represented in Fig. 1(e). The specific surface area of the AC obtained is 408.8 m^2/g. This may be due to the type of raw biomass utilized, carbonization method, and amount of activating agent used. Fig. 1(f) represents the pore size distribution, and pore volume calculated by the BJH method is 0.073 cc/g, and the average pore width is 19.159 nm.

FE-SEM images were used to depict the morphological characteristics of AC. Fig. 2(a, b) represents the morphology of the AC before activation, and images indicate that before activation, no porous geometry was observed; only sheets-like structures were present in the sample.

Fig. 2(c, d) represents FE-SEM images for AC, indicating that the AC sample has porous surface morphologies with a homogenous sponge-like branching structure and inter-connected pores. The elemental distribution of elements using energy-dispersive X-ray (EDX) analysis and chemical characterization of synthesized AC are shown in Fig. 2 (e, f). EDX spectra represent that the AC sample contains mainly carbon and oxygen.

CV curves are shown in Fig. 3(a). The CV curves have a quasi-rectangular shape, signifying the development of an electrical double layer in an aqueous electrolyte [10]. The shape of the CV curves depicts that the working electrode achieved fast ion diffusion resulting in smooth charge propagation. The GCD curves at current densities ranging from 1 to 10 Ag^{-1} are shown in Fig. 3(b). Eq. (1) was used to calculate the specific capacitance.

$$C_s = \frac{I \times t}{m \times \Delta V} \quad (1)$$

In the left-hand side of the above equation, the C_s represent the specific capacitance, and in the right-hand side of the above equation, I, t, ΔV, and m represent the current, discharge time, potential window, and mass of the working electrode, respectively.

The GCD analysis illustrates high reversibility and coulombic efficiency, which is essential for a supercapacitor electrode. Under a constant current density of 1 Ag^{-1}, the AC electrode has a specific capacitance of 204 Fg^{-1}. The Nyquist plots of AC electrodes are shown in Fig. 3(c). The inset of Fig. 3(c) shows the equivalent circuit obtained using simulation circuit fit with internal resistance (R_Ω), charge transfer resistance (R_{ct}), Warburg impedance (Z_w), and double-layer capacitance (C_{dl}) [11]. The AC electrode's internal resistance was determined to be 1.6 Ω. The resistance of the working electrode is found lower due to the free electron present in the graphitized structure. The value of charge-transfer resistance (R_{ct}) was 2.67 Ω using an electrochemical circuit fit. The nearly vertical line in the low-frequency range affects ion diffusion within the system, which is attributed to the AC electrode's high porosity and surface area explained by Warburg impedance [12]. The electrochemical stability of the prepared electrode was assessed using GCD tests for 10,000 cycles (current density 10 A/g); as shown in Fig. 3(d), the specific capacitance slightly decreased and retained up to 83.9 %. The prepared electrode shows a remarkable energy density of 28.3 Wh kg^{-1} at 499 Wkg^{-1}, based on the total mass of the active material [13] as shown in Fig. 3(f).

4. Conclusions

The AC-based supercapacitor electrode has a high specific capacitance of 204 Fg^{-1} at 1 Ag^{-1} and shows a remarkable energy density of 28.3 $Whkg^{-1}$ at 499 Wkg^{-1} of power density. The specific capacitance decreases and retains 83.9 % up to 10,000 cycles. The study depicts that the waste (walnut shell) is a highly appropriate precursor due to its cheap, maintainable, and environmentally safe for fabricating AC for the electrochemical supercapacitor electrode to overcome the energy-related problem that we are facing.

CRediT authorship contribution statement

Raman Devi: Writing – original draft, Investigation. **Vinay Kumar:** Resources, Writing – review & editing, Supervision. **Sunil Kumar:** Conceptualization, Validation. **Avnish Kumar Sisodiya:** Writing – review & editing. **Ajay Kumar Mishra:** Methodology. **Anushree Jatrana:** Formal analysis, Data curation. **Ashwani Kumar:** Resources, Writing – review & editing. **Paul Singh:** Data curation, Writing – review & editing.

Declaration of Competing Interest

The authors declare that they have no known competing financial interests or personal relationships that could have appeared to influence the work reported in this paper.

Data availability

No data was used for the research described in the article.

Acknowledgment

We are grateful to the Department of Materials Science and Engineering, NIT, Hamirpur, H.P., for providing necessary ads for characterization tools.

Appendix A. Supplementary data

Supplementary data to this article can be found online at https://doi.org/10.1016/j.matlet.2023.133830.

References

[1] A.S. Winata, H. Devianto, R.F. Susanti, Materials Today Proceedings 44 (2021) 3268–3272.
[2] R. Kötz, M.J. Carlen, Electrochimica acta 45 (2000) 2483–2498.
[3] Y. Kumar, S. Rawal, B. Joshi, S.A. Hashmi, Journal of Solid State Electrochemistry 23 (2019) 667–692.
[4] L.L. Zhang, X.S. Zhao, Chemical Society Reviews 38 (2009) 2520–2531.
[5] P. González-García, Renewable and Sustainable Energy Reviews 82 (2018) 1393–1414.
[6] X. Du, W. Zhao, Y. Wang, C. Wang, M. Chen, T. Qi, C. Hua, M. Ma, Bioresource Technology 149 (2013) 31–37.
[7] X. Jiang, F. Guo, X. Jia, S. Liang, K. Peng, L. Qian, Ionics 26 (2020) 3655–3668.
[8] R. Devi, V. Kumar, S. Kumar, A. Jatrana, A. Agrawal, P. Singh, ECS Transactions 107 (2022) 7979–7986.
[9] P. Makuła, M Pacia & amp, W, Macyk, The Journal of Physical Chemistry Letters 9 (2018) 6814–6817.
[10] A. Rajapriya, S. Keerthana, C. Viswanathan, N. Ponpandian, Journal of Alloys and Compounds 859 (2021), 157771.
[11] E. Taer, A.M. Miftah, S.M. Widya, R. Taslim, Journal of Applied Engineering Science 19 (2021) 162–171.
[12] H. Yang, Y. Tang, X. Huang, L. Wang, Q. Zhang, Journal of Materials Science: Materials in Electronics 28 (2017) 18637–18645.
[13] L. Chunyang, W. Wenzhuo, W. Peng, Z. Weibin, W. Jing, C. Yuhui, F. Lijun, Z. Yusong, W. Yuping, W. Huang, Advanced Science 6 (1) (2019) 1801665.